Journal of Applied Polymer Science

Effect of the melting temperature on the crystallization behavior of a poly(L-lactide)/poly(D-lactide) equimolar mixture

Yongai Yin,[1] Yan Song,[1] Zujiang Xiong,[1] Xiuqin Zhang,[2] Sicco de Vos,[3] Ruyin Wang,[4] Cornelis A. P. Joziasse,[3] Guoming Liu,[1] Dujin Wang[1]

[1]Beijing National Laboratory for Molecular Sciences, Key Laboratory of Engineering Plastics, Institute of Chemistry, Chinese Academy of Sciences, Beijing 100190, China

[2]School of Materials Science and Engineering, Beijing Institute of Fashion Technology, Beijing 100029, China

[3]Corbion Purac, P.O. Box 21 4200AA, Gorinchem, The Netherlands

[4]Corbion Purac China, Unit 08-09, 30F, 6088 Humin Road, Minhang District, Shanghai 201100, China

Correspondence to: X. Zhang (E-mail: clyzxq@bift.edu.cn)

ABSTRACT: The effect of the final melting temperature (T_f) on the crystallization of poly(L-lactide) (PLLA)/poly(D-lactide) (PDLA) was studied via a combination of differential scanning calorimetry, wide-angle X-ray scattering, polarized optical microscopy, and Fourier transform infrared (FTIR) spectroscopy. We observed that a residual stereocomplex (SC) crystal induced the formation of SC crystals during cooling from a T_f (230°C) just above the melting peak of the SC crystals. On cooling from a T_f (240°C) just above the endset temperature of SC crystal melting [$T_m(S)(E)$], the possible order structure and the strong interchain interaction promoted the preferential crystallization of SC crystals; this enhanced the formation of α crystals. During cooling from a T_f (≥250°C) far above $T_m(S)(E)$, the crystallization peaks of α and SC crystals converged. The FTIR results indicated that the residual SC crystals, possible ordered structure, and interchain interactions in the melt might have been the key factors for the different crystallization of PLLA/PDLA. © 2015 Wiley Periodicals, Inc. J. Appl. Polym. Sci. **2016**, *133*, 43015.

KEYWORDS: biocompatibility; biodegradable; crystallization; polyesters

Received 9 June 2015; accepted 7 October 2015

DOI: 10.1002/app.43015

INTRODUCTION

Polylactide (PLA) is commonly synthesized by the ring-opening polymerization of lactide.[1] According to the chirality of monomers (L-lactide, D-lactide, or mesolactide), PLA has three forms, that is, poly(L-lactide) (PLLA), poly(D-lactide) (PDLA), and poly(L,D-lactide). Under different preparation conditions, PLLA or PDLA can form various crystal modifications (α, β, γ, and α′).[2–6] Among them, the α crystal is the most stable form and could be formed by the traditional melt or solution crystallization of PLLA or PDLA. In 1987, Ikada *et al.*[7] first reported that a new crystal, called a *stereocomplex (SC) crystal*, was produced by the equimolar mixing of PLLA and PDLA through melt or solution blending. The melting temperature of the SC crystal [$T_m(S)$] was approximately 50°C higher than that of the α crystal in PLLA or PDLA. Therefore, PLLA/PDLA blends with pure SC crystals provide a potential possibility for developing thermally resistant PLA-based materials.[8–10]

A complicated relationship between the α and SC crystal in the PLLA/PDLA blend was found under certain conditions.[11–16] Anderson *et al.*[15] found that the nucleation efficiency of 3 wt % PDLA could reach 100%. The half-crystallization time for PLLA at 140°C decreased from 17 min to less than 1 min, and the PDLA showed a nucleation efficiency even higher than that of talc. Tsuji and coworkers[17,18] also found that the nucleation density and crystallization rate of PLLA could be significantly improved by the addition of a small amount of SC crystals. If SC crystals were abundantly formed in the PLLA/PDLA blends, the subsequent crystallization of the neat PLLA chains took place in spaces confined by the SC crystal network. This led to a lower crystallization rate and decreased crystallinity of homo(α) crystals.[19]

The final melting temperature (T_f) is one of the vital factors for polymer crystallization.[20–22] Numerous studies have reported that the crystallization behavior of the asymmetric PLLA/PDLA blend showed a dependence on T_f.[23,24] Narita and coworkers[25–27] found that nonmelted or recrystallized SC crystals had a higher accelerating effect on the formation of α crystals in PLLA compared to the partially melted SC crystals. The crystallization behavior of the symmetric PLLA/PDLA blends under different T_f values were also reported. When the molecular weights of PLLA and PDLA

were low, there was no formation of α crystals for all of the T_f's investigated.[23,28] Therefore, these studies focused on the effect of T_f on the crystallization of SC crystals in symmetric PLLA/PDLA blends with low molecular weight. It was found that the crystallization rate of SC crystals decreased with increasing T_f or prolonging melting time.[23,28] However, with increasing molecular weight of PLLA or PDLA, α crystals could be also formed, accompanied with SC crystals in symmetric PLLA/PDLA blends.[29,30] Under these conditions, the effect of T_f on SC and α crystals and the complicated relationship between the two kinds of crystals have not been explored systematically in the symmetric PLLA/PDLA blend.

In this study, PLLA and PDLA with high molecular weights were selected. The crystallization behavior of the symmetric PLLA/PDLA blend under different T_f conditions was systematically studied; this included the formation of SC and α crystals under different T_f's. The differences of the initial melting structure of the PLLA/PDLA blend at different T_f values were studied by *in situ* Fourier transform infrared (FTIR) spectroscopy. The aim was to explain the intrinsic reason for the different crystallization behaviors.

EXPERIMENTAL

Materials and Sample Preparation

PLLA (optical purity > 99%, weight-average molecular weight = 82 kg/mol, number-average molecular weight = 48 kg/mol, polydispersity index = 1.72) and PDLA (optical purity > 98%, weight-average molecular weight = 79 kg/mol, number-average molecular weight = 43 kg/mol, polydispersity index = 1.83) were kindly provided by Corbion Purac. They had a glass-transition temperature of about 61°C and a melting temperature (T_m) of 174°C [differential scanning calorimetry (DSC); 10°C/min].

The PLLA/PDLA solution was prepared by dissolution of the compounds into chloroform at a 1:1 weight ratio with vigorous stirring for 2 h. The solution was cast on a culture dish followed by the evaporation of chloroform at room temperature for 1 day. The obtained films were further vacuum-dried for 24 h to remove the residual solvent at 80°C.

Measurements

DSC. The melting and crystallization behavior of the PLLA/PDLA blend was examined with a TA Instrument DSC Q2000. The instrument was calibrated with indium before measurement. The samples were protected under a nitrogen atmosphere during measurement. The films were heated to different T_f values (i.e., 230, 240, 250, and 260) at a rate of 30°C/min (the first heating), annealed at the same T_f for 1 min, cooled to 50°C at a rate of 5°C/min (the first cooling), and then reheated to 260°C at a rate of 30°C/min (the second heating).

Wide-Angle X-ray Scattering (WAXS). *In situ* X-ray scattering measurements were carried out at the 1W2A beamline in the Beijing Synchrotron Radiation Facility. The wavelength (λ) of the radiation source was 1.54 Å. To make sure that the samples were heated evenly, they were wrapped with thin aluminum foil. The samples were placed on a Linkam TST 350 hot stage (Linkam Scientific Instruments, Ltd., United Kingdom), heated to different T_f values at a rate of 30°C/min, annealed at the same T_f for 1 min, and then cooled to 50°C at a rate of 5°C/min. Scattering patterns were collected by a MAR CCD (MAR-USA) detector with a resolution of 2048 × 2048 pixels (79 × 79 μm^2) during cooling. The image acquisition time was 17 s. The sample-to-detector distance was 224.76 mm for WAXS. All of the X-ray patterns were corrected by background scattering, air scattering, and beam fluctuation.

The one-dimensional (1D) diffraction intensity for each 2θ was obtained by integration over the azimuthal range (60–120°) of the 2D diffraction images. To estimate the fraction of different phases, the WAXS intensity profiles were deconvoluted into several Gaussian profiles to represent all of the visible scattering peaks and the amorphous halo.[12,31] The relative fraction of different phases of the samples was estimated according to the following:

$$X_\alpha = \frac{I_\alpha}{I_\alpha + I_{SC} + I_{amor}} \quad (1)$$

$$X_{sc} = \frac{I_{SC}}{I_\alpha + I_{SC} + I_{amor}} \quad (2)$$

$$X = X_\alpha + X_{SC} \quad (3)$$

In eqs. (1) and (2), I_α, I_{SC}, and I_{amor} stand for the integral intensities of the peaks of the α crystals, SC crystals and amorphous phase, respectively.

Polarized Optical Microscopy (POM). POM observation was performed on an Olympus BX50 polarizing optical microscope equipped with a digital camera. The temperature was controlled by a Linkam LT350 hot stage (Linkam Co.). The samples were heated to different T_f values at a rate of 30°C/min, annealed at the same T_f for 1 min, and then cooled to 50°C at a rate of 5°C/min in a nitrogen atmosphere.

FTIR Spectroscopy. FTIR spectra were recorded with a Nicolet 6700 spectrometer equipped with an MCT detector in transmission mode. The spectra were collected at a resolution of 4 cm^{-1}, and an average over 16 scans was obtained. The film was obtained by the casting of a chloroform solution of PLLA/PDLA (2 g/dL) on KBr pellets and then drying for 30 min. The film was heated to 200°C at a rate of 30°C/min and then continuously heated to 260°C at a rate of 5°C/min.

RESULTS AND DISCUSSION

Nonisothermal Crystallization Behavior during Cooling from Different T_f Values

Figure 1 shows the 1D WAXS intensity profiles and DSC heating scan of the as-cast PLLA/PDLA film. From WAXS, the reflections of (110), (300/030), and (203) assigned to the SC crystals were observed at 2θ values of 11.9, 20.6, and 23.8°,[4,32] respectively. A weak reflection originated from the α crystals was observed at a 2θ of 16.6°.[33] The result indicates that the original film was mainly composed of SC crystals and very few α crystals. The DSC result shows that the weak melting peak of the α crystals appeared around 157°C. The melting peak of the SC crystals was observed at around 220°C; this was in agreement with the previous report[7] and suggested that the equal proportional blending favored the formation of SC crystals.[34] According to the melting range of SC crystals, 230, 240, 250, and 260°C were chosen as T_f's to explore the influence of different initial melt states on the subsequent

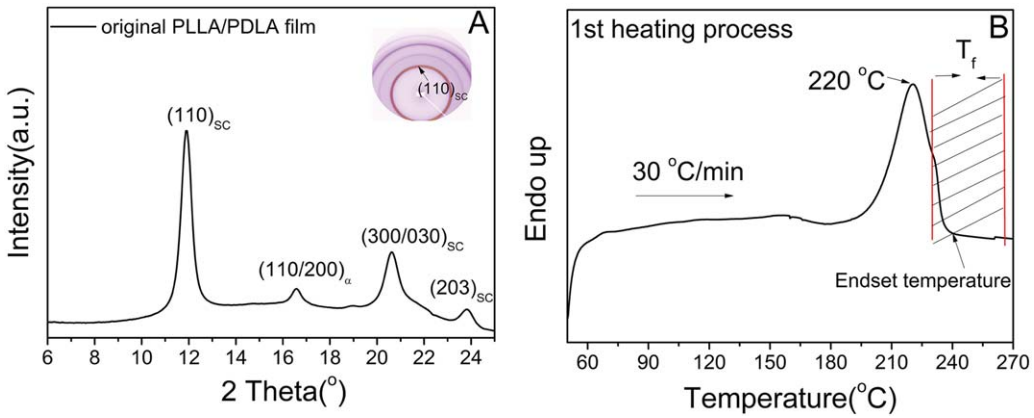

Figure 1. (A) 1D WAXS intensity profiles and (B) DSC heating thermograph of the as-cast PLLA/PDLA film. The DSC heating rate was 30°C/min. α, α crystals; SC, SC crystals. [Color figure can be viewed in the online issue, which is available at wileyonlinelibrary.com.]

crystallization behavior of the PLLA/PDLA blends. As shown in Figure 1(B), 230°C was the temperature just above the melting peak of the SC crystals, where the crystals were partially melted; 240°C was the temperature just above the endset temperature of the SC crystal melting peak, where all of the crystals were melted completely; and 250 and 260°C were the temperatures far above the endset temperature of the SC crystal melting peak, where all of the crystals melted completely.

The DSC scans of the PLLA/PDLA blends are presented in Figure 2. The corresponding extracted parameters are summarized in Table I. When T_f was 230°C, the PLLA/PDLA blend crystallized quickly on cooling, and only an exothermic crystallization peak appeared at about 220°C. Because the crystallization temperature was higher than the melting peak of α crystals, it was assigned to the crystallization of SC crystals. During the corresponding second heating process, an obvious endothermic peak was observed around 241°C; this suggested that only SC crystals were formed under these conditions. It was noteworthy that a shoulder peak was observed at about 230°C, and this was assigned to the annealing peak.[35] When T_f was 240°C, two exothermic peaks appeared at 199 and 138°C in the PLLA/PDLA blend during cooling, respectively. In the subsequent heating scan, two endothermic peaks (175 and 226°C) were observed; these corresponded to the melting of α crystals and SC crystals. When T_f was 250°C, only a crystallization peak appeared at about 107°C; this implied that the crystallization temperature and rate of the PLLA/PDLA blend decreased. When T_f increased to 260°C, the exothermic peak became broad, the enthalpy was low, and the crystallization ability of the PLLA/PDLA blend was depressed. As shown in Table I, the crystallization temperature of the SC crystals in the PLLA/PDLA blend with a T_f of 240 or 250°C shifted to a lower temperature compared to that in the blend with a T_f of 230°C. We observed that $T_m(S)$ during the second heating decreased with increasing T_f (Figure 3). As the T_m of the polymer crystallites depended on the lamellar thickness, the decrease in $T_m(S)$ suggested that the lamellar thickness of the SC crystals formed during cooling decreased with increasing T_f. Additionally, the melting enthalpies of SC crystals [$\Delta H_m(S)$] decreased with increasing T_f from 230 to 250°C. With a T_f higher than 250°C, the $\Delta H_m(S)$ values in the PLLA/PDLA blend increased again because of the possible thermal degradation (Figure 3).

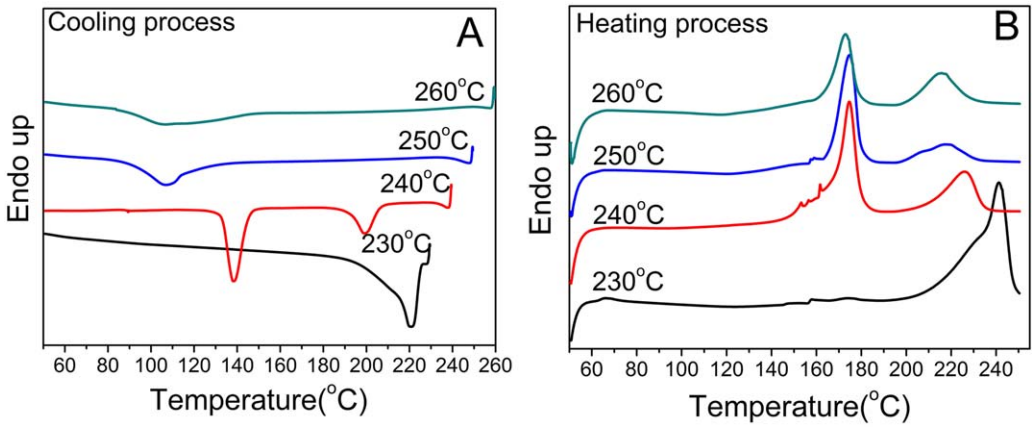

Figure 2. DSC thermographs of the PLLA/PDLA blends during the (A) first cooling from different T_f values to 50°C and (B) second heating from 50 to 260°C. The cooling and the heating rates were 5 and 30°C/min, respectively. α, α crystals; SC, SC crystals. [Color figure can be viewed in the online issue, which is available at wileyonlinelibrary.com.]

Table I. Thermal Properties of the PLLA/PDLA blends during the First Cooling and the Second Heating

	T_{mc} (°C)		ΔH_{mc} (J/g)					
Sample	$T_{mc}(H)$ (°C)	$T_{mc}(S)$ (°C)	$\Delta H_{mc}(H)$ (J/g)	$\Delta H_{mc}(S)$ (J/g)	$T_m(H)$ (°C)	$\Delta H_m(H)$ (J/g)	$T_m(S)$ (°C)	$\Delta H_m(S)$ (J/g)
PLLA/PDLA-230°C	—	220	—	56.3	—	—	241	56.1
PLLA/PDLA-240°C	138	199	35.4	16.5	175	39.6	226	19.6
PLLA/PDLA-250°C	107		37.2		175	27.3	217	10.6
PLLA/PDLA-260°C	106		33.2		173	19.3	215	15.9

T_{mc}, thermal crystallization temperature; ΔH_{mc} and ΔH_m, enthalpies of thermal crystallization and melting, respectively; (*H*) and (*S*) indicate the PLLA homocrystal (α) and the SC crystals, respectively.

Evolution of the Crystalline Structure during Cooling from Different T_f Values

To investigate the crystallization behavior of α and SC crystals in the PLLA/PDLA blends during cooling, *in situ* X-ray analysis was carried out. 1D WAXS intensity profiles of the PLLA/PDLA blends during cooling from different T_f values are shown in Figure 4.

After the PLLA/PDLA blend was annealed at 230°C for 1 min, weak crystal reflections of (110) and (030/300) assigned to the SC crystals were observed (as shown in Figure 4). During cooling, the reflection intensities of the SC crystals increased, and no α crystal reflections were observed; this was in accordance with the results of DSC. Apart from the sample with a T_f of 230°C, the intensity profiles of the samples with other T_f's displayed the diffusion halos; this showed that all of the crystals disappeared in the blends under these T_f's. Upon cooling, the onset crystallization temperatures of the SC crystals [$T_{c,onset}(S)$] were about 224, 148, and 148°C for the blends with T_f's of 240, 250, and 260°C, respectively. Correspondingly, the onset crystallization temperatures of the α crystals [$T_{c,onset}(\alpha)$] were about 144, 130, and 130°C, respectively. In addition, when T_f was 240°C, the diffraction profiles in Figure 4 verified that the higher temperature exothermic peak in the DSC cooling thermograph belonged to the crystallization of SC crystals, and the lower one was assigned to the α crystals. When T_f was higher than 240°C, the effects of T_f on $T_{c,onset}(\alpha)$ and $T_{c,onset}(S)$ in the PLLA/PDLA blends became weaker with increasing T_f.

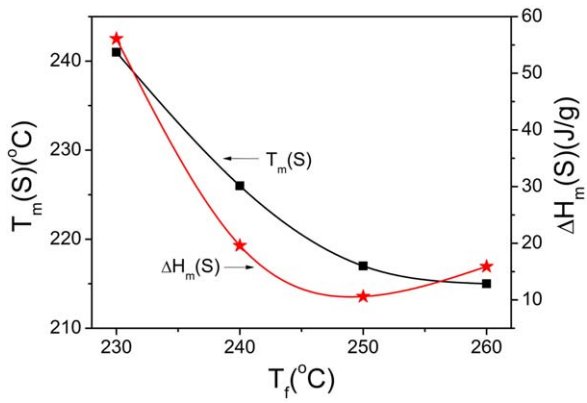

Figure 3. $T_m(S)$ and $\Delta H_m(S)$ of the SC crystals in the PLLA/PDLA blends during the second heating from 50 to 260°C as a function of T_f. [Color figure can be viewed in the online issue, which is available at wileyonlinelibrary.com.]

The fractions of the α crystals and SC crystals in the PLLA/PDLA blends with different T_f values were estimated by the deconvolution of the WAXS intensity profiles. The 2θ range of 6–26° was fitted by nine Gaussian type peaks: two amorphous peaks, three SC peaks, and four α crystal peaks. The amorphous halo was fitted by two peaks at 2θ values of 12.6 and 15.3°. The contents of SC crystals and α crystals and the total crystallinity of the PLLA/PDLA blend during cooling from different T_f values are plotted in Figure 5. When the PLLA/PDLA blend was cooled from 230°C, only SC crystals were formed, and the total crystallinity was the highest, reaching about 62%. During cooling from 240°C, SC crystals started to crystallize at about 224°C; the crystallization leveled off at about 180°C. The final content of SC crystals was about 28%. Subsequently, α crystals were formed at about 144°C. The content of α crystals remained constant at about 100°C and reached approximately 30%. Because of the formation of α crystals, the total crystallinity of the PLLA/PDLA blend rapidly increased to about 58%. When T_f was higher than 240°C, the fractions of SC crystals in the samples decreased and were about 10%. The content of α crystals in the PLLA/PDLA blend with a T_f of 250°C (~30%) was higher than those with a T_f of 260°C (~27%). Therefore, the total crystallinity of the PLLA/PDLA blend with a T_f of 250°C was higher than that with a T_f of 260°C.

In previous literature, it was reported that the preferentially formed SC crystals in the PLLA/PDLA blends affected the following formation of α crystals.[13,36] The content of SC crystals at $T_{c,onset}(\alpha)$ for the PLLA/PDLA blends cooled from different T_f values is summarized in Table II. As described previously, after annealing at 230°C for 1 min, the residual SC crystals induced the crystallization of SC crystals. The content of SC crystals reached about 60%. The high-content SC crystals hindered the crystallization of α crystals. For the PLLA/PDLA blend with a T_f of 240°C, the SC crystals crystallized at about 224°C, and the content of SC crystals was about 25% when α crystals in the PLLA/PDLA blend started to crystallize at about 144°C. The existing SC crystals promoted the formation of α crystals, and their crystallization temperature was about 138°C (Figure 2); this was higher than the 110°C crystallization temperature of α crystals for pure PLA.[37] When T_f increased to 250°C or greater, $T_{c,onset}(\alpha)$ decreased to about 130°C. At this temperature, the content of SC crystals was about 3–6%; this suggested that the SC crystals crystallized incompletely. According to the crystallization temperature shown in Figure 2(A), the nucleating effect of the SC crystals on α crystals was depressed. Therefore, in combination with the results of DSC, we speculated that the

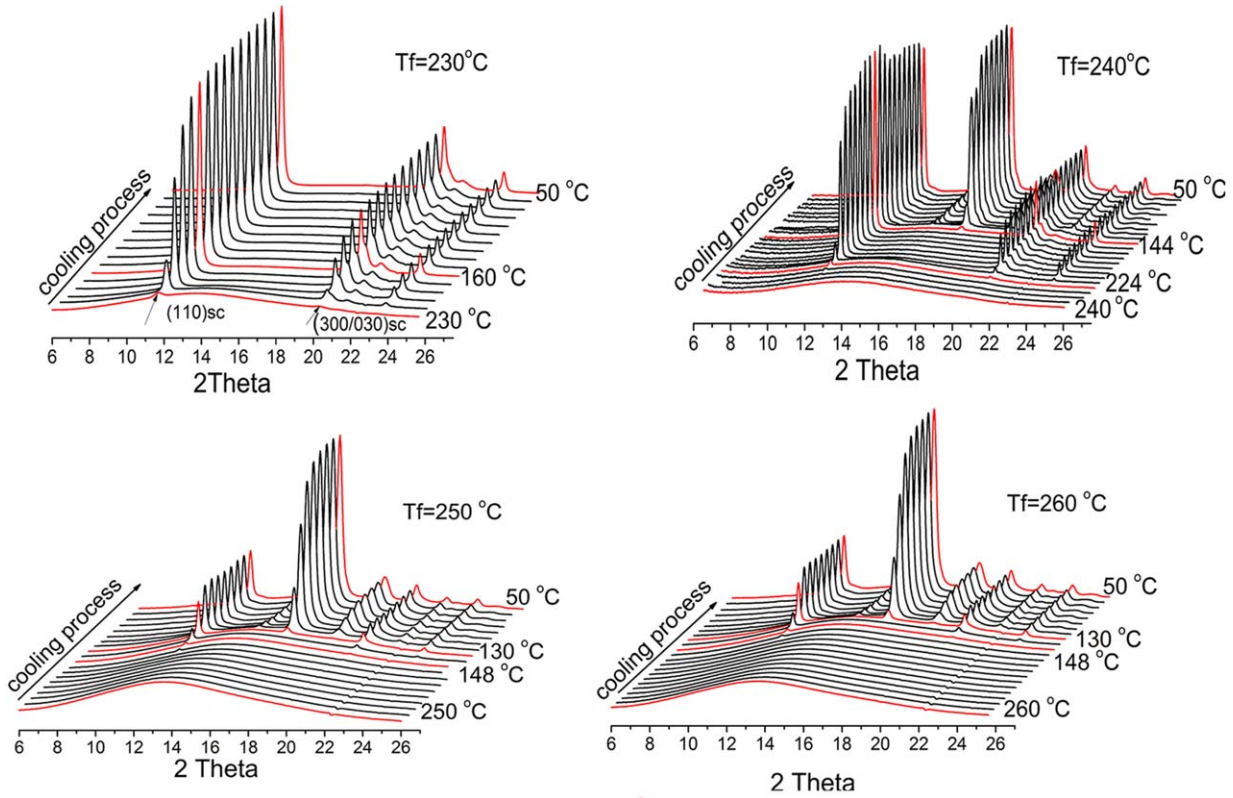

Figure 4. X-ray diffraction profiles of the PLLA/PDLA films during cooling from different T_f values. The cooling rate was 5°C/min. [Color figure can be viewed in the online issue, which is available at wileyonlinelibrary.com.]

crystallization of the α crystals depended on the crystallization temperature and the crystallinity of SC crystals.

Crystalline Morphologies of the PLLA/PDLA Blends during Cooling

The development of the crystalline morphologies for the PLLA/PDLA blends cooled from different T_f values to 50°C is shown in Figure 6. When T_f was 230°C, no crystals were observed at the beginning. When the temperature decreased to about 210°C, a large amount of SC crystals were formed rapidly. When T_f was 240°C, no crystals existed in the melt. A larger number of small crystals appeared with decreasing temperature to about 190°C; this indicated that the PLLA/PDLA blend still had a high nucleation density. However, when T_f was 250°C, the nucleation density of the PLLA/PDLA blend decreased. As the temperature decreased to about 150°C, some small spherulites were formed. After they were cooled to 50°C, spherulites with different sizes were observed in the final morphology. When T_f increased to 260°C, a very small amount of spherulites was observed when the temperature decreased to 145°C. Furthermore, the growth of spherulites was slow, and finally, the sizes were small. The POM results also showed that the crystallization ability of the PLLA/PDLA blends decreased with increasing T_f.

In Situ FTIR Analysis of the PLLA/PDLA Blends during Heating to Different T_f Values

FTIR spectroscopy is a common method for characterizing the polymer structure; it is very sensitive to polymer conformation

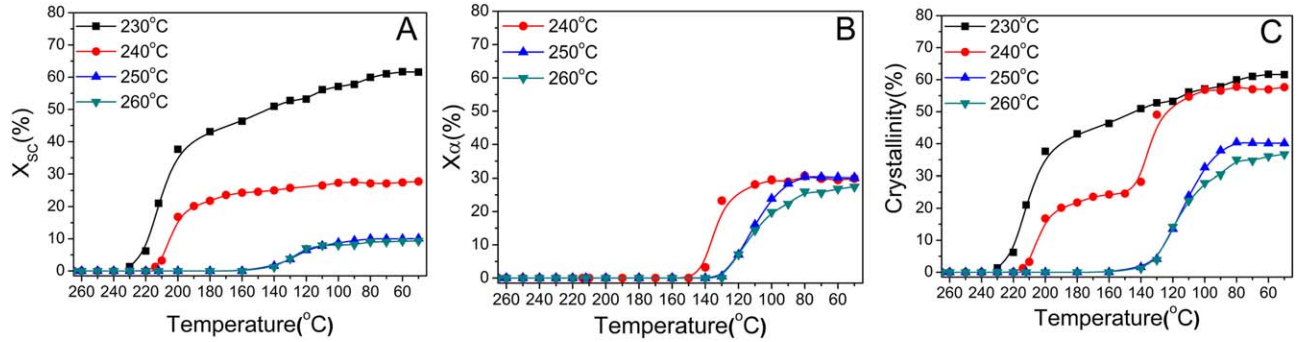

Figure 5. Variation of the (A) SC crystals and (B) α crystals and total crystallinity of the PLLA/PDLA blends during cooling from different T_f values (calculated from WAXS data). [Color figure can be viewed in the online issue, which is available at wileyonlinelibrary.com.]

Table II. $T_{c,onset}$(SC) and Content of the SC Crystals at $T_{c,onset}(\alpha)$ (X_{SC}) for the PLLA/PDLA Blends Cooled from Different T_f Values

T_f (°C)	$T_{c,onset}$(S) (°C)[a]	$T_{c,onset}(\alpha)$ (°C)[a]	X_{SC} (%)
230	230	—	61.6
240	224	144	25.0
250	148	130	3.6
260	148	130	3.4

[a] $T_{c,onset}(S)$ and $T_{c,onset}(\alpha)$ in the PLLA/PDLA blends cooling from different T_f values, respectively.

and changes in the molecular region.[38,39] The melting process of the polymer was evaluated by the tracing of the variation of the characteristic bands to explore the differences in its melting structure.[40,41]

There existed a variety of conformation and crystalline sensitive bands for PLLA.[42–44] Difference spectra are often used to eliminate the highly overlapped bands.[45] The evolution of the initial melting states of the PLLA/PDLA blend with different T_f values was investigated by *in situ* FTIR spectroscopy [Figure 7(A)]. The bands at about 1454 and 1210 cm^{-1} were attributed to the asymmetric deformation mode of CH_3, and the asymmetric vibrations of C—O—C groups were linked with asymmetric CH_3 rocking vibrations, respectively. When the ordered structure of molecules formed in the polymer systems, the 1200 cm^{-1} band turned into two bands at 1210 and 1180 cm^{-1} because of dipole–dipole coupling; this was caused by the interchain packing of —CH_3 groups in the crystal unit cell of PLLA.[39] Therefore, the intensity variation of the band at about 1210 cm^{-1} was correlated with the interchain interaction.[38] According to the literature,[46] SC crystals with a 3_1 helical conformation had a characteristic band at about 908 cm^{-1}; this was related to the coupling of C—C backbone stretching with the CH_3 rocking mode. Except for the characteristic band at 908 cm^{-1}, the bands at 1039 cm^{-1} indicated that the stretching vibrations of the C—CH_3 group also acted as a characteristic band of SC crystals.[45] Because of the small intensity change of the characteristic band at 908 cm^{-1}, the intensity change at 1039 cm^{-1} represented the melt behavior of SC crystals during heating. On the other hand, the characteristic band of the amorphous phase was about 1256 cm^{-1}. The difference spectra showed that the crystals melted gradually with increasing temperature. The intensities of the bands related to crystalline structure

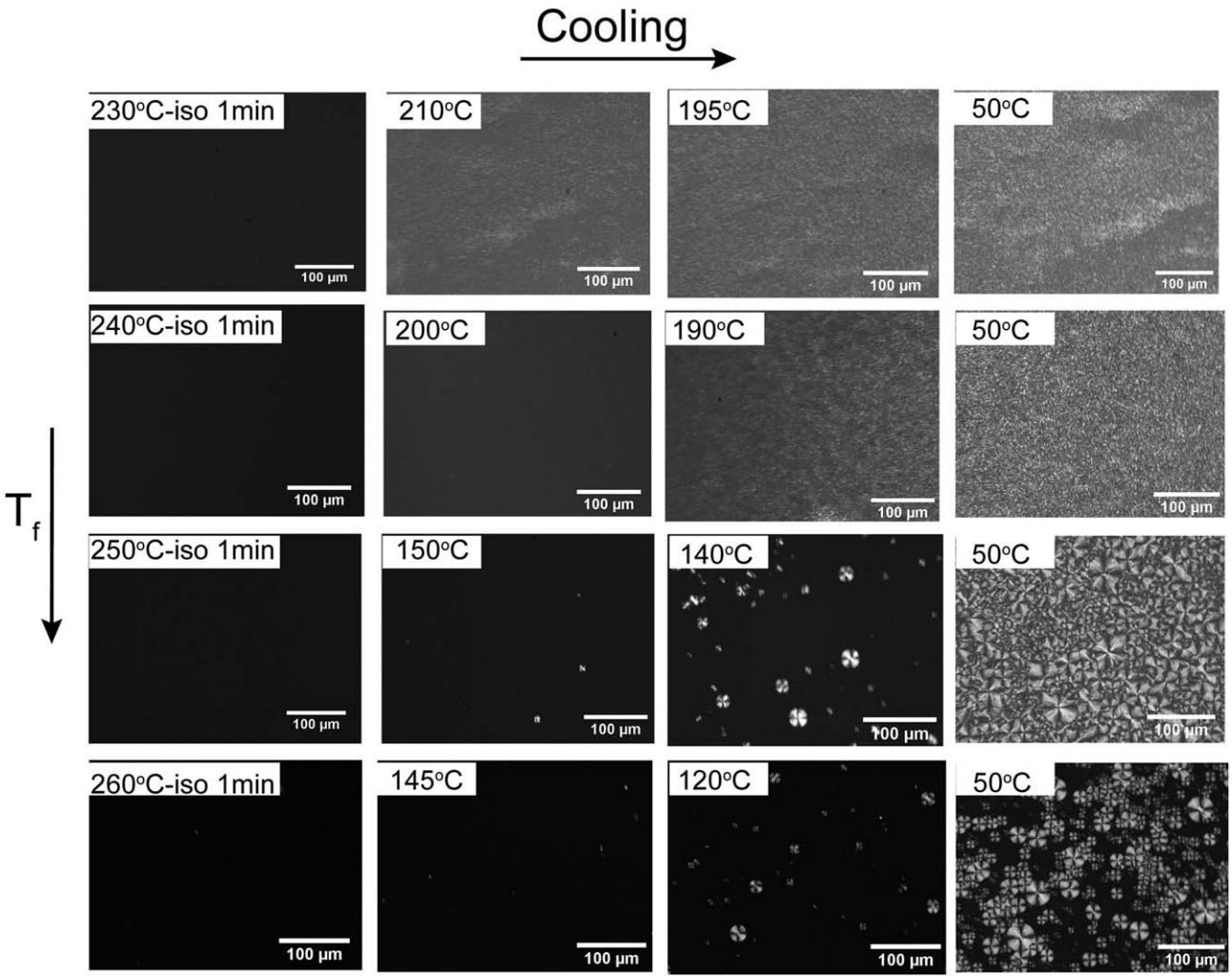

Figure 6. POM micrographs of the crystalline morphologies for the PLLA/PDLA blends during cooling from different T_f values. The cooling rate was 5°C/min.

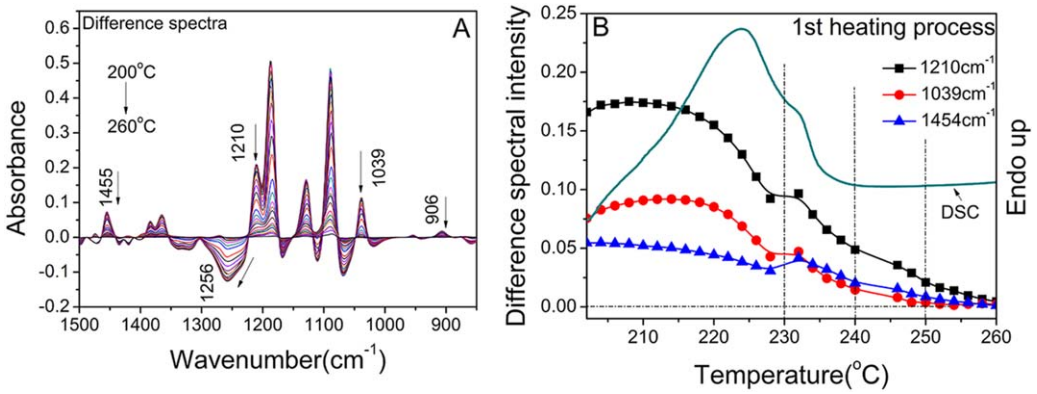

Figure 7. (A) Difference spectra of the FTIR spectra in the range 1500–900 cm^{-1} collected during the first heating process (200–270°C) and (B) variation of the difference spectral intensities of 1454, 1210, and 1039 cm^{-1} and corresponding DSC curve of the PLLA/PDLA blend. The heating rate was 5°C/min. [Color figure can be viewed in the online issue, which is available at wileyonlinelibrary.com.]

decreased, and those related to the amorphous phase increased. The intensity of the band at about 1256 cm^{-1} increased, and the intensity of the band at about 1039 cm^{-1} decreased; this showed that the SC crystals were melting.

The quantitative analysis of the characteristic bands with increasing temperature is summarized in Figure 7(B). On the basis of the melting of SC crystals in the blend, T_f is divided into three parts:

1. At a T_f value just above $T_m(S)$ (230°C), the existence of 1039 cm^{-1} indicated that residual SC crystals still remained. According to the results of DSC and X-ray data, surviving SC crystals induced the crystallization of SC crystals. This process may have been similar to the annealing treatment of the original SC crystals at high temperature.
2. At a T_f value just above the endset temperature of SC crystal melting (240°C), although the DSC and X-ray results showed that the SC crystals were melted, the existence of 1039 cm^{-1} indicated that some possible order structure may have remained in the melt. Moreover, the intensity of 1210 cm^{-1} was high; this suggested relatively strong interchain interaction and favored the formation of the stable nuclei. Therefore, the high nucleation rate of PLLA/PDLA with a T_f of 240°C resulted from the remaining order structure and the high interchain interaction. According to the theory of self-nucleation,[21,22,35] some residual crystal fragments, which could not be detected by DSC and WAXS, could act as nucleation sites to induce polymer crystallization. These self-nuclei may have arisen from the residual segmental order in the melt (i.e., a melt memory effect) or the precursor for polymer crystallization. The crystallization of SC crystals in the PLLA/PDLA blend at a T_f of 240°C was similar to that described by self-nucleation theory.
3. At T_f value far above the endset temperature of SC crystal melting (≥250°C), the ordered structure was completely melted. The decrease in interchain interaction (1454 and 1210 cm^{-1}) led to a weak ability to form stable nuclei. SC crystals in the PLLA/PDLA blend crystallized from the sporadic nuclei at low temperature with high supercooling; this was accompanied by the formation of α crystals. Finally, the crystallization ability of PLLA/PDLA decreased. According to the previous results, we speculated that the different initial melting states of the blends (i.e., residual SC crystals, residual segmental order, and interchain interaction) resulted in the different crystallization behavior of SC or α crystals in PLLA/PDLA blends.

CONCLUSIONS

In this study, the effect of T_m on the crystallization of the PLLA/PDLA blends was studied. When the sample was cooled from T_f, where the SC crystals were partially melted, the residual crystal nuclei were well-dispersed from the partial melting of the existing crystals, and then, only SC crystals were formed. As the sample was cooled from T_f, where the SC crystals were just melted, the possible small size ordered structure and the strong interchain interactions promoted the preferential formation of SC crystals. The formed SC crystals with the appropriate content had a high nucleation efficiency on the subsequent crystallization of α crystals. During cooling from the highest T_f, the possible residual segmental order disappeared, and the interchain interactions were weak. The crystallization of SC crystals in the PLLA/PDLA blend was depressed. The crystallization peaks of the SC and α crystals converged, and the crystallization ability of the PLLA/PDLA blend decreased. The research results may provide theoretical guidance for the selection of processing temperatures of PLA materials and the regulation of the PLA crystalline structure.

ACKNOWLEDGMENTS

This work was financially supported by the National Natural Science Foundation of China (contract grant number 51203170), the Beijing Training Project for the Leading Talents in Science and Technology (contract grant number LJ201305), the New Century Excellent Talents in University (contract grant number NCET-12-0601), and the Beijing Municipal Natural Science Foundation (contract grant number KZ201310012014). The authors thank the Beijing Synchrotron Radiation Facility for kindly providing beam time.

REFERENCES

1. Anders, S.; Mikael, S. In Poly(lactic acid): Synthesis, Structure, Properties, Processing, and Application; Auras, R. A.; Lim, L T.; Selke, S. E.; Tsuji, H. John Wiley & Sons, Inc., Hoboken, New Jersey, **2010**; Chapter 3, p 34.
2. De Santis, P.; Kovacs, A. J. *Biopolymers* **1968**, *6*, 299.
3. Eling, B.; Gogolewski, S.; Pennings, A. *Polymer* **1982**, *23*, 1587.
4. Cartier, L.; Okihara, T.; Ikada, Y.; Tsuji, H.; Puiggali, J.; Lotz, B. *Polymer* **2000**, *41*, 8909.
5. Zhang, J.; Duan, Y.; Sato, H.; Tsuji, H.; Noda, I.; Yan, S.; Ozaki, Y. *Macromolecules* **2005**, *38*, 8012.
6. Liu, G.; Zhang, X.; Wang, D. *Adv. Mater.* **2014**, *26*, 6905.
7. Ikada, Y.; Jamshidi, K.; Tsuji, H.; Hyon, S. H. *Macromolecules* **1987**, *20*, 904.
8. Ahmed, J.; Varshney, S. K.; Janvier, F. *J. Therm. Anal. Calorim.* **2014**, *115*, 2053.
9. Zhu, J.; Na, B.; Lv, R. H.; Li, C. *Polym. Int.* **2014**, *63*, 1101.
10. Shao, J.; Xiang, S.; Bian, X. C.; Sun, J. R.; Li, G.; Chen, X. S. *Ind. Eng. Chem. Res.* **2015**, *54*, 2246.
11. Schmidt, S. C.; Hillmyer, M. A. *J. Polym. Sci. Part B: Polym. Phys.* **2001**, *39*, 300.
12. Xiong, Z.; Liu, G.; Zhang, X.; Wen, T.; de Vos, S.; Joziasse, C.; Wang, D. *Polymer* **2013**, *54*, 964.
13. Wei, X. F.; Bao, R. Y.; Cao, Z. Q.; Yang, W.; Xie, B. H.; Yang, M. B. *Macromolecules* **2014**, *47*, 1439.
14. Pan, P.; Han, L.; Bao, J.; Xie, Q.; Shan, G.; Bao, Y. *J. Phys. Chem. B* **2015**, *119*, 6462
15. Anderson, K. S.; Hillmyer, M. A. *Polymer* **2006**, *47*, 2030.
16. Bao, R. Y.; Yang, W.; Jiang, W. R.; Liu, Z. Y.; Xie, B. H.; Yang, M. B. *J. Phys. Chem. B* **2013**, *117*, 3667.
17. Tsuji, H.; Takai, H.; Saha, S. K. *Polymer* **2006**, *47*, 3826.
18. Tsuji, H.; Takai, H.; Fukada, N.; Takikawa, H. *Macromol. Mater. Eng.* **2006**, *291*, 325.
19. Sun, J.; Yu, H.; Zhuang, X.; Chen, X.; Jing, X. *J. Phys. Chem. B* **2011**, *115*, 2864.
20. Castillo, R. V.; Muller, A. J.; Raquez, J. M.; Dubois, P. *Macromolecules* **2010**, *43*, 4149.
21. Schneider, S.; Drujon, X.; Lotz, B.; Wittmann, J. C. *Polymer* **2001**, *42*, 8787.
22. Fillon, B.; Wittmann, J. C.; Lotz, B.; Thierry, A. *J. Polym. Sci. Part B: Polym. Phys.* **1993**, *31*, 1383.
23. Sun, J.; Shao, J.; Huang, S.; Zhang, B.; Li, G.; Wang, X.; Chen, X. *Mater. Lett.* **2012**, *89*, 169.
24. Yamane, H.; Sasai, K. *Polymer* **2003**, *44*, 2569.
25. Narita, J.; Katagiri, M.; Tsuji, H. *Polym. Int.* **2013**, *62*, 936.
26. Narita, J.; Katagiri, M.; Tsuji, H. *Macromol. Mater. Eng.* **2013**, *298*, 270.
27. Narita, J.; Katagiri, M.; Tsuji, H. *Macromol. Mater. Eng.* **2011**, *296*, 887.
28. He, Y.; Xu, Y.; Wei, J.; Fan, Z.; Li, S. *Polymer* **2008**, *49*, 5670
29. Tsuji, H.; Hyon, S. H.; Ikada, Y. *Macromolecules* **1991**, *24*, 5651.
30. Tsuji, H. *Macromol. Biosci.* **2005**, *5*, 569.
31. Stoclet, G.; Seguela, R.; Lefebvre, J. M.; Rochas, C. *Macromolecules* **2010**, *43*, 7228.
32. Sawai, D.; Tsugane, Y.; Tamada, M.; Kanamoto, T.; Sungil, M.; Hyon, S. H. *J. Polym. Sci. Part B: Polym. Phys.* **2007**, *45*, 2632.
33. Brizzolara, D.; Cantow, H. J.; Diederichs, K.; Keller, E.; Domb, A. J. *Macromolecules* **1996**, *29*, 191.
34. Tsuji, H.; Horii, F.; Hyon, S. H.; Ikada, Y. *Macromolecules* **1991**, *24*, 2719.
35. Lorenzo, A. T.; Arnal, M. L.; Sánchez, J. J.; Müller, A. J. *J. Polym. Sci. Part B: Polym. Phys.* **2006**, *44*, 1738.
36. Rahman, N.; Kawai, T.; Matsuba, G.; Nishida, K.; Kanaya, T.; Watanabe, H.; Okamoto, H.; Kato, M.; Usuki, A.; Matsuda, M.; Nakajima, K.; Honma, N. *Macromolecules* **2009**, *42*, 4739.
37. Yin, H. Y.; Wei, X. F.; Bao, R Y.; Dong, Q. X.; Liu, Z. Y.; Yang, W.; Xie, B.-H.; Yang, M. B. *ACS Sustain. Chem. Eng.* **2015**, *3*, 654.
38. Yang, C. F.; Huang, Y. F.; Ruan, J.; Su, A. C. *Macromolecules* **2012**, *45*, 872.
39. Zhang, J.; Tsuji, H.; Noda, I.; Ozaki, Y. *J. Phys. Chem. B* **2004**, *108*, 11514.
40. Zhu, X.; Yan, D. *Macromol. Chem. Phys.* **2001**, *202*, 1109.
41. Zhu, X.; Yan, D.; Yao, H.; Zhu, P. *Macromol. Rapid Commun.* **2000**, *21*, 354.
42. Xing, Q.; Zhang, X.; Dong, X.; Liu, G.; Wang, D. *Polymer* **2012**, *53*, 2306.
43. Xu, J. Z.; Chen, T.; Yang, C. L.; Li, Z. M.; Mao, Y. M.; Zeng, B. Q.; Hsiao, B. S. *Macromolecules* **2010**, *43*, 5000.
44. Krikorian, V.; Pochan, D. J. *Macromolecules* **2005**, *38*, 6520.
45. Zhang, J.; Sato, H.; Tsuji, H.; Noda, I.; Ozaki, Y. *Macromolecules* **2005**, *38*, 1822.
46. Zhang, J.; Tashiro, K.; Tsuji, H.; Domb, A. J. *Macromolecules* **2007**, *40*, 1049.